

# Composites with extremal thermal expansion coefficients

O. Sigmund<sup>a)</sup> and S. Torquato<sup>b)</sup>

Princeton Materials Institute and Department of Civil Engineering and Operations Research,  
Princeton University, Princeton, New Jersey 08540

(Received 22 July 1996; accepted for publication 12 September 1996)

We design three-phase composites having maximum thermal expansion, zero thermal expansion, or negative thermal expansion using a numerical topology optimization method. It is shown that composites with effective negative thermal expansion can be obtained by mixing two phases of positive thermal expansions with a void phase. We also show that there is no mechanistic relationship between negative thermal expansion and negative Poisson's ratio. © 1996 American Institute of Physics. [S0003-6951(96)04147-2]

Materials with extreme or unusual thermal expansion behavior are of interest from both a technological and fundamental standpoint. Examples include materials with zero thermal expansion, maximum thermal expansion or force, and negative (i.e., minimum) thermal expansion. Heretofore, however, a systematic procedure to design such materials has been lacking.

Zero thermal expansion materials are needed in structures subject to temperature changes such as space structures, bridges, and piping systems. Materials with large thermal displacement or force can be employed as "thermal" actuators. A fastener made of a negative thermal expansion material, upon heating, can be inserted easily into a hole. Upon cooling it will expand, fitting tightly into the hole.

A negative thermal expansion material has the counterintuitive property of contracting upon heating. Existing materials with negative expansions include glasses in the titania-silica family<sup>1</sup> at room temperature  $T$ , silicon and germanium<sup>2</sup> at very low  $T$  ( $<100$  K), and  $ZrW_2O_8$  for a wide range of  $T$ .<sup>3</sup> Materials with directional negative expansion coefficients at room temperature include Kevlar, carbon fibers, plastically deformed (anisotropic) Invar (Fe-Ni alloys),<sup>4</sup> and certain molecular networks.<sup>5</sup>

In this letter we use a topology optimization procedure<sup>6</sup> to determine the distribution of two different bulk material phases and a void phase to design 2D composites with extremal or unusual thermal expansion behavior. Three phases are used (as opposed to two phases) since one can achieve composite properties beyond those of the individual components.<sup>7</sup> An interesting question (that we answer below) is whether there is a mechanistic relationship between negative thermal expansion and negative Poisson's ratio.<sup>8</sup> We first describe briefly the optimization procedure (see Ref. 6 for details) and then present results for specific design examples.

Assuming 2D linear elasticity, perfect interface bonding, uniform temperature distribution, and isotropic material properties, thermoelastic behavior of materials is described by the constitutive relations

$$\boldsymbol{\sigma} = \mathbf{C}(\boldsymbol{\epsilon} - \boldsymbol{\alpha}\Delta T) = \mathbf{C}\boldsymbol{\epsilon} - \boldsymbol{\beta}\Delta T, \quad (1)$$

where

$$\mathbf{C} = \frac{E}{1-\nu^2} \begin{pmatrix} 1 & \nu & 0 \\ \nu & 1 & 0 \\ 0 & 0 & \frac{1-\nu}{2} \end{pmatrix}, \quad (2)$$

$\boldsymbol{\sigma}$  and  $\boldsymbol{\epsilon}$  are the stress and strain tensors,  $E$  and  $\nu$  are the Young's modulus and Poisson's ratio, and  $\Delta T$  is the temperature change. The thermal strain tensor  $\boldsymbol{\alpha}$  is the resulting strain of a material allowed to expand freely; the thermal stress tensor  $\boldsymbol{\beta} = \mathbf{C}\boldsymbol{\alpha}$  is the stress per degree K in the material constrained not to expand. For a three-phase composite, relation (1) is valid on a local scale (with subscripts 0, 1, and 2 appended to the properties) and the macroscopic scale (with subscript \* appended to effective properties).

The topology optimization procedure used here is a modification<sup>9</sup> of standard methods<sup>10</sup> (see also Ref. 6). The design domain is the periodic base cell and is initialized by discretizing it into 3600 finite elements. One seeks the optimal distribution of the two base materials and the void phase, such that the objective function (e.g., effective properties) is minimized, with constraints on the moduli and symmetry. The optimization procedure solves a sequence of finite element problems followed by changes in material type of each of the finite elements, based on sensitivities of the objective function and constraints.

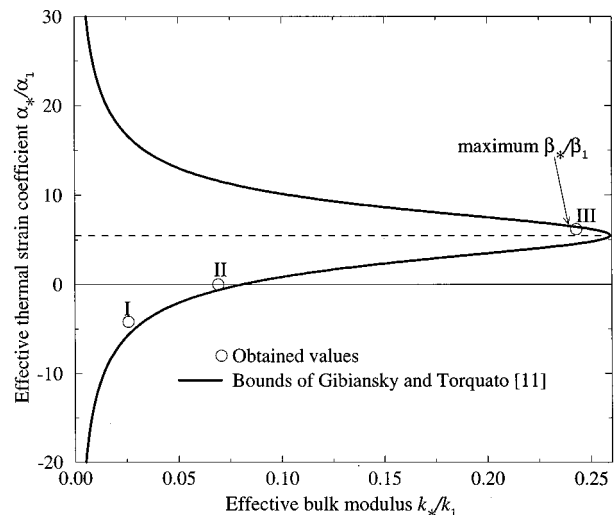


FIG. 1. Bounds for three-phase design examples I-III that correspond to microstructures shown in Fig. 2

<sup>a)</sup> Present and permanent address: Department of Solid Mechanics, Technical University of Denmark, DK-2800 Lyngby, Denmark. Electronic mail: sigmund@fam.dtu.dk

<sup>b)</sup> Electronic mail: torquato@matter.princeton.edu

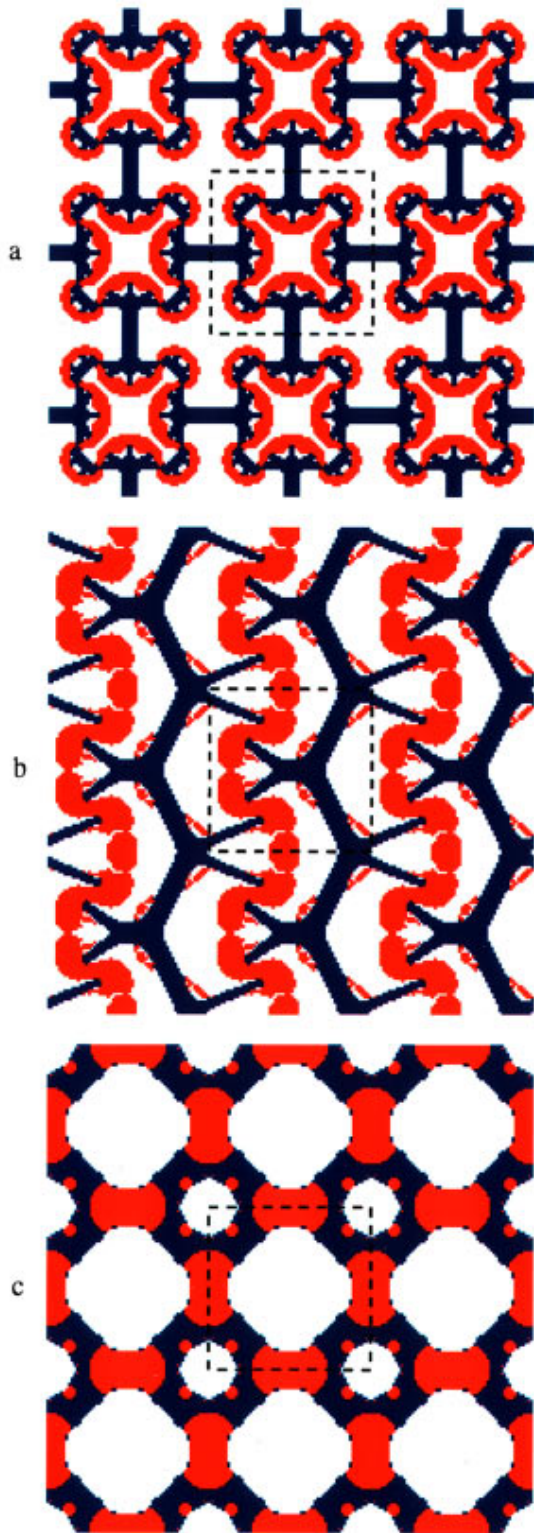


FIG. 2. Optimal microstructures composed of hypothetical phases (red is high expansion phase, blue is low expansion phase and white is void). (a) I: Minimization of  $\alpha_*$ ; (b) II: Maximization of  $k_*$  for zero thermal expansion; and (c) III: Maximization of  $\beta_*$ . Structures correspond to circles labeled I-III in Fig. 1.

To benchmark the algorithm, we first check to see how close we can approach new rigorous bounds on the effective isotropic thermal expansion coefficients for three-phase composites.<sup>11</sup> The phase data are taken as  $E_2/E_1=1$ ,  $\nu_1=\nu_2=0.3$ ,  $\alpha_2/\alpha_1=10$ ,  $c_0=0.5$ , and  $c_1=c_2=0.25$ . The volume fractions  $c_i$  are held fixed to compare with the

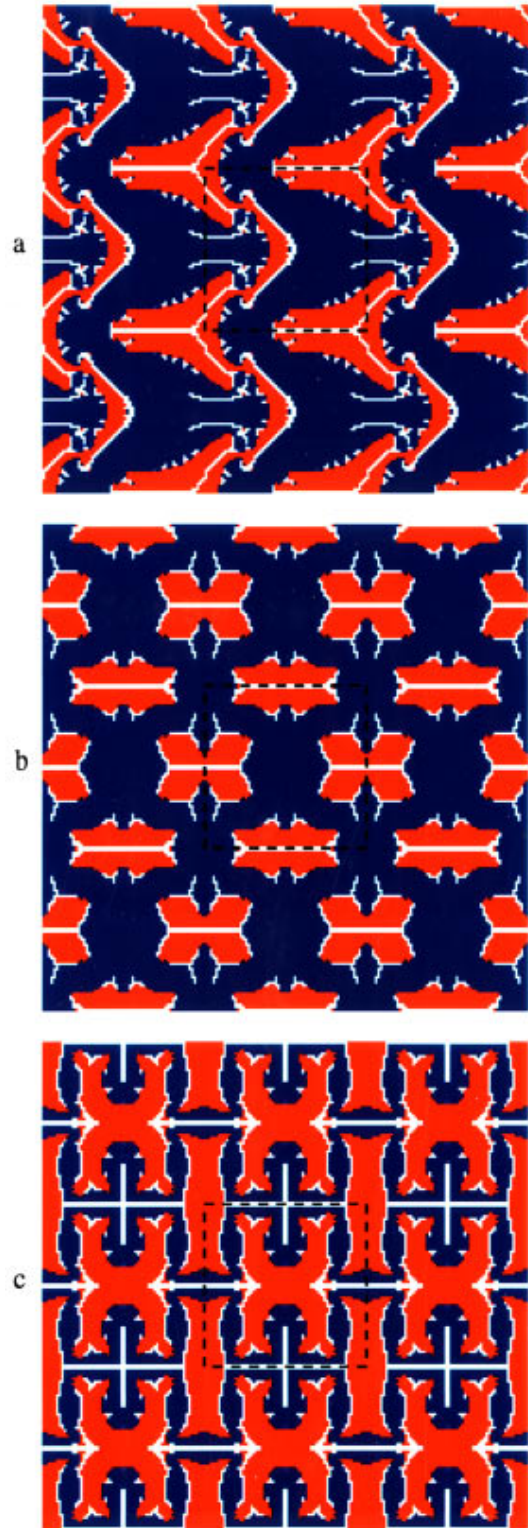


FIG. 3. Optimal microstructures composed of Invar (blue), nickel (red), and void (white). (a) IV: Minimization of  $\beta_*$ ; (b) V: Maximization of contractive vertical stress; and (c) VI: Maximization of vertical strain.

bounds, which are most naturally expressed in terms of the effective bulk modulus  $k_* = E_*/2(1 - \nu_*)$ .

Consider the following three hypothetical design examples constrained to be elastically isotropic: I: minimization of the isotropic thermal strain coefficient  $\alpha_*/\alpha_1$  with lower bound constraint on effective bulk modulus  $k_*$  given as 10% of the upper bound bulk modulus value and four-fold

TABLE I. Thermoelastic parameters for optimal microstructures made of Invar (phase 1) and nickel (phase 2). Note that for the isotropic example IV,  $\beta_* = E_* \alpha_* / (1 - \nu_*) = 2k_* \alpha_*$ .

Material	$\alpha_*$ $\mu\text{m}/(\text{mK})$	$E_*$ GPa	$\nu_*$	$\beta_*$ kPa/K	$c_1/c_2$
Invar	0.8	150	0.31	174	1/0
Nickel	13.4	200	0.31	3884	0/1
IV	-4.97	14.8	0.055	-77.6	0.60/0.28
V	5.42/-4.68	69.9/29.5	0.059/0.025	372/-129	0.60/0.30
VI	23.4/35.0	1.09/5.00	-.135/-0.621	2.01/174	0.38/0.46

geometric symmetry; II: maximization of  $k_*/k_1$  for fixed zero thermal expansion ( $\alpha_*/\alpha_1=0$ ) and horizontal reflection symmetry; III: maximization of isotropic thermal stress coefficient  $\beta_*/\beta_1$  and fourfold symmetry. The effective properties [ $\alpha_*/\alpha_1, k_*/k_1$ ] are plotted in Fig. 1, and the corresponding three by three arrays of the optimal base-cell topologies are shown in Fig. 2. The designed composite properties are seen to be very close to the new bounds, thus validating the procedure.<sup>12</sup> Figure 1 shows that there is a tradeoff between extremizing thermal strain coefficients on the one hand and ending up with a stiff material on the other.

When allowing low bulk moduli, the main mechanism behind the negative thermal expansion is the reentrant (non-convex) cell structure having bimaterial components. When heated, the bimaterial interfaces of design example I bend and make the cell contract, similar to the behavior of negative Poisson's ratio materials.<sup>8</sup> If a higher effective bulk modulus is specified, as in II, the intricate bimaterial mechanisms are less pronounced resulting in a less extreme expansion ( $\alpha_*=0$ ). Finally, maximizing the expansive stress, as in example III, results in a structure without bimaterial mechanisms, where the high expansion (red) phase is arranged such that it maximizes the horizontal and vertical expansion.

To design real new materials with extreme thermal expansion, the two base materials should be of similar stiffness but widely differing thermal expansions. Two materials fulfilling this requirement are isotropic Invar (Fe-36%Ni) and nickel, which have Young's moduli of 150 and 200 GPa, respectively, thermal expansion coefficients of 0.8 and 13.4  $\mu\text{m}/(\text{mK})$ , respectively, and Poisson's ratios of 0.31 for both. Consider the following design examples: IV: minimization of the isotropic thermal stress coefficient  $\beta_*$  and horizontal reflection symmetry; V: minimization of the vertical thermal stress  $(E_*)_2(\alpha_*)_{22}$  and horizontal and vertical reflection symmetry; and VI: maximization of the vertical strain  $(\alpha_*)_{22}$  with the constraint on the vertical Young's modulus  $(E_*)_2 \geq 5$  GPa and horizontal and vertical reflection symmetry. For examples IV-VI, the phase volume fractions  $c_i$  are unconstrained, allowing for a wider range of minimum and maximum values.

The resulting optimal topologies are shown in Fig. 3 and the corresponding effective properties are listed in Table I. As the optimal structures of design examples V and VI are anisotropic, Table I lists two numbers: for  $\alpha_*$ ,  $E_*$ , and  $\beta_*$  these are the associated horizontal and vertical components, respectively, and for  $\nu_*$  these are the components  $(\nu_{12})_*$  and  $(\nu_{21})_*$ .<sup>6</sup>

To overcome the positive thermal expansion of other surrounding materials, we seek to maximize the contraction force, i.e., minimize  $\beta_*$  as in example IV. The isotropic vertical contraction stress (per degree K) of example IV is  $E_* \alpha_* = -73.6$  kPa/K. Relaxing the isotropy requirement, as in example V, reduces this directional value to  $(E_*)_2(\alpha_*)_{22} = -137.7$  kPa/K.

The isotropic negative thermal expansion materials in examples I and IV both have positive Poisson's ratios (0.52 and 0.06, respectively), showing that there is no mechanistic relationship between negative thermal expansion and negative Poisson's ratio. In example VI we see again that anisotropy can lead to very high directional expansion coefficients. The vertical coefficient  $(\alpha_*)_{22}$  of example VI is 2.6 times higher than for solid nickel, but at the cost of a low vertical Young's modulus.

Our optimally designed materials can be built (with micron-scale cells) using stereolithography or surface micro-machining techniques.<sup>13</sup> It will be interesting to study whether lessons learned from this continuum analyses can be exploited to optimally design materials at the molecular level. Elsewhere we will apply the method, which is not limited to 2D, to optimally design 3D piezocomposites for use as actuators or sensors.

We thank L. Gibiansky, R. Lakes, M. Bendsøe, P. Pedersen, I. Aksay, and G. Scherer for useful discussions. This work was supported by the ARO/MURI Grant No. DAAH04-95-1-0102 (O.S. and S.T.) and Denmark's Technical Research Council (O.S.).

<sup>1</sup>P. C. Schultz and H. T. Smyth, in *Amorphous Materials* (edited by R. Douglas and B. Ellis (Wiley, New York, 1970).

<sup>2</sup>H.-M. Kagaya and T. Soma, *Solid State Commu.* **85**, 617 (1993).

<sup>3</sup>T. A. Mary, J. S. O. Evans, T. Vogt, and A. W. Sleight, *Science* **272**, 90 (1996).

<sup>4</sup>G. Hausch, R. Bächer, and J. Hartmann, *Physica B* **161**, 22 (1989).

<sup>5</sup>R. H. Baughman and D. S. Galvão, *Nature* **365**, 735 (1993).

<sup>6</sup>O. Sigmund and S. Torquato, *J. Mech. Phys. Solids* (to be published).

<sup>7</sup>R. Lakes (private communication).

<sup>8</sup>Negative Poisson's ratio materials expand laterally when pulled axially and can be made by processing foams with reentrant cells; see for example R. Lakes, *Science* **235**, 1038 (1987).

<sup>9</sup>O. Sigmund, Ph.D. thesis, Technical University of Denmark, 1994; *Int. J. Solids Structures* **31**, 2313 (1994).

<sup>10</sup>M. P. Bendsøe and N. Kikuchi, *Comp. Meth. Appl. Mech. Eng.* **71**, 197 (1988); M. P. Bendsøe, *Methods for the Optimization of Structural Topology* (Springer, Berlin, 1995).

<sup>11</sup>L. V. Gibiansky and S. Torquato (unpublished).

<sup>12</sup>One can get even closer to the bounds using finer discretizations; this was not done for computing-time reasons.

<sup>13</sup>U. D. Larsen, O. Sigmund, and S. Bouwstra, in *IEEE International Workshop on Micro Electro Mechanical Systems*, 1996.